

Evolutionary and functional insights into Leishmania META1: evidence for lateral gene transfer and a role for META1 in secretion

Puri *et al.*

RESEARCH ARTICLE

Open Access

Evolutionary and functional insights into *Leishmania* META1: evidence for lateral gene transfer and a role for META1 in secretion

Vidhi Puri¹, Aneesh Goyal^{1,3}, Rajan Sankaranarayanan¹, Anton J Enright² and Tushar Vaidya^{1*}

Abstract

Background: *Leishmania* META1 has for long been a candidate molecule for involvement in virulence: META1 transcript and protein are up-regulated in metacyclic *Leishmania*. Yet, how META1 contributes to virulence remains unclear. We sought insights into the possible functions of META1 by studying its evolutionary origins.

Results: Using multiple criteria including sequence similarity, nucleotide composition, phylogenetic analysis and selection pressure on gene sequence, we present evidence that META1 originated in trypanosomatids as a result of a lateral gene transfer of a bacterial heat-inducible protein, HslJ. Furthermore, within the *Leishmania* genome, META1 sequence is under negative selection pressure against change/substitution. Using homology modeling of *Leishmania* META1 based on solved NMR structure of HslJ, we show that META1 and HslJ share a similar structural fold. The best hit for other proteins with similar fold is MxiM, a protein involved in the type III secretion system in *Shigella*. The striking structural similarity shared by META1, HslJ and MxiM suggests a possibility of shared functions. Upon structural superposition with MxiM, we have observed a putative hydrophobic cavity in META1. Mutagenesis of select hydrophobic residues in this cavity affects the secretion of the secreted acid phosphatase (SAP), indicating META1's involvement in secretory processes in *Leishmania*.

Conclusions: Overall, this work uses an evolutionary biology approach, 3D-modeling and site-directed mutagenesis to arrive at new insights into functions of *Leishmania* META1.

Background

Leishmaniasis is a spectrum of parasitic disease caused by *Leishmania* spp. protozoa, transmitted to its mammalian host by bite of an infected female sand fly vector. The clinical manifestations of the disease range from the potentially fatal visceral disease caused by *L. donovani* complex (*L. donovani* and *L. infantum*) to disfiguring, but self curing cutaneous form caused by *L. major* in the Old World and *L. amazonensis* and *L. mexicana* in the New World. Within the sand fly, *Leishmania* exists as an extracellular, flagellated form and gets transformed into an intracellular, sessile amastigote in phagolysosome of the macrophages. The role of many molecules like GP63 [1-5], lipophosphoglycan [6-12], cysteine proteases [13-15] etc. that are differentially expressed in the two

developmental stages of the parasite have been studied for their involvement in adaptation of the parasite in such disparate environments and enhancing virulence of the parasite. A lot more remains to be learnt, including the functions, of many such virulence factors. Understanding the mechanistic details of function of virulence factors will help us develop novel intervention strategies against the parasite and the disease.

META1 was one such gene identified in *L. major*, found to be conserved across the *Leishmania* genus. Both transcript and protein was found to be up-regulated in the metacyclic stage of promastigotes. The META1 protein was found to localize surrounding the flagellar pocket in *L. major* stationary phase promastigotes [16]. On META1 overexpression in *L. amazonensis*, parasites were found to be more virulent than wild-type [17]. Another gene in *Leishmania*, also up-regulated in metacyclic promastigotes is named META2, and contains three META domains and a calpain-like domain at the

* Correspondence: tvaidya@ccmb.res.in

¹Centre for Cellular and Molecular Biology, Council for Scientific and Industrial Research, Uppal Road, Hyderabad - 500 007, Andhra Pradesh, India
Full list of author information is available at the end of the article

carboxy terminus [18]. META (PF03724) is currently described as a small domain family of unknown function in *Leishmania* META1 and in bacterial proteins, hypothetically secreted/implicated in motility. However, apart from some of its developmental expression and its suggested role in virulence, the precise functions of META1 in the parasite remain unknown.

In order to understand *META1*'s function, we investigated its relationship with its near homologs in other organisms. Based on several criteria, we have been able to establish in this study that *META1* of *Leishmania* is a homolog of a bacterial gene for a heat shock inducible protein, *hslJ* that has been transferred by an ancient lateral gene transfer event between bacteria and a trypanosomatid ancestor. We have highlighted similarities in various characteristics of the two proteins like their relatedness to pathogenicity/virulence, heat inducible expression and also shown by homology modeling that they are not only evolutionarily linked but structurally similar as well. Furthermore, our homology modeling identified yet another structural homolog MxiM, a secretin pilot protein of *Shigella flexneri*, which is involved in that pathogen's type III secretion system. Based on structural homology between META1 & MxiM and subsequent mutagenesis, we have identified a putative hydrophobic cavity in *Leishmania* META1 that seems to be important for function of META1 and indicates a role for META1 in *Leishmania* secretory processes.

Results

Sequence similarity searches

The META1 sequence is highly conserved across the *Leishmania* genus [16]. Based on this high degree of conservation and the convenient accessibility of *L. major* genome sequence and other related resources over those for other *Leishmania* species, all of our bioinformatics analyses have used *L. major* META1 as the representative species. We began our study by using BLASTP to search for homologs of META1 protein against the NCBI NRDB. Homologs of META1 were found in all other *Leishmania* species and Trypanosomes (Additional file 1).

Since BLASTP search failed to detect any functionally characterized homolog within or outside the Trypanosomatidae family, a PSI-BLAST search was performed against NCBI NRDB. This search yielded hits beyond the trypanosomatids as early as the second iteration. Interestingly, these significant hits were all homologs of the heat shock inducible protein HslJ from bacteria. Table 1 lists representative hits after 3 iterations. All sequence homologs of META1 (trypanosomatid as well as bacterial) are characterized by the presence of at least one META domain. Although there is a low direct pairwise sequence identity of 25% between META1 and HslJ (Figure 1),

bacterial HslJ is currently the closest relative of *Leishmania* META1 outside the family Trypanosomatidae. The most likely explanation for this unusual phyletic relationship is that *META1* in trypanosomatids originated as a result of a lateral gene transfer (LGT) event from bacteria.

Anomalous nucleotide composition

Most genomes have distinct overall GC content and the genes in their genome are fairly similar in base composition and patterns of codon usage. A laterally transferred gene continues to carry imprints of its origin and ancestry whilst residing in its current recipient genome. Such 'foreign genes' can be identified by their unusual sequence characteristics vis a vis the recipient genome [19-21]. GC content at first and third codon positions and synonymous codon usage are generally used for such analysis. ORFs are identified as atypical if their GC contents at first and third codon positions (GC_1 & GC_3 respectively) are two or more standard deviations (SDs) higher or lower than the respective means for all genes in that genome. Our analysis revealed that the total GC content of *L. major* META1 is 54%, which is 6.3 SD lower than the average of the total GC content of all genes in *L. major* genome. In addition, *LmjMETA1* has a GC_1 content of 48.67% (15.8 SD lower than GC_1 of all genes in *L. major* genome) and a GC_3 content of 77% (within the range of SD for GC_3 of *L. major* genome), as summarized in Figure 2A. GC content anomaly results establish that *META1* nucleotide composition is distinct from the overall *Leishmania* genome and therefore, is possibly of foreign origin.

Codon adaptation index (CAI), on the other hand, gives an account of similarity of synonymous codon usage to that of a standard set of highly expressed genes for that organism. Thus, for a native gene CAI is high and for a gene of exogenous origin CAI value is low. As part of CAI determination, we analyzed a set of other genes for reference along with *META1* (Additional file 2). The genes that were included: Amastin & GP63 (specific to trypanosomatids), Hexokinase & Ribosomal Protein S8 (present in all taxa), α -Tubulin (a pan-eukaryotic structural protein) and PTR-1 & Coproporphyrinogen, previously predicted to be laterally transferred in *L. major* from bacteria [22]. *META1*, PTR-1 and Coproporphyrinogen all have low CAI values when compared to the other reference genes (Figure 2B), suggesting again, that *META1* is of exogenous origin. We also carried out a similar analysis on META1 homologs in *T. cruzi* (Additional file 3); where once again the CAI of the META homologs is lower than that of other *Trypanosoma* genes (RP S8 and α -Tubulin). These analyses, and the striking frequency of bacterial HslJ hits, point to bacterial *hslJ* being the exogenous source of *META1* into trypanosomatids.

Table 1 List of bacterial HslJ hits obtained from PSI-BLAST search after 3 iterations for *Lmj*META1 against non-redundant NCBI database

Species Name	Description	Accession	E-value
<i>Cyanothece</i> sp. PCC 7822	Protein of unknown function, DUF306 Meta and HslJ	ZP_03153678.1	7e ⁻²³
<i>Beutenbergia cavernae</i> DSM 12333	Protein of unknown function, DUF306 Meta and HslJ	YP_002881157.1	2e ⁻¹⁶
<i>Tolomonas auensis</i> DSM 9187	Protein of unknown function, DUF306 Meta and HslJ	YP_002892522.1	2e ⁻⁷
<i>gamma proteobacterium</i> HTCC5015	Conserved hypothetical protein	ZP_05061049.1	2e ⁻⁶
<i>Roseobacter</i> sp. AzwK-3b	Hypothetical protein RAZWK3B_01740	ZP_01901204.1	5e ⁻⁶
<i>Sphingopyxis alaskensis</i> RB2256	Protein of unknown function, DUF306 Meta and HslJ	YP_617096.1	1e ⁻⁵
<i>Alcanivorax</i> sp. DG881	Conserved domain protein	ZP_05041611.1	2e ⁻⁵
<i>Vibrionales bacterium</i> SWAT-3	Hypothetical protein VSWAT3_19198	XP_844891.1	2e ⁻⁵
<i>Roseovarius</i> sp. TM1035	Probable secreted protein containing HslJ-like protein	XP_844900.1	2e ⁻⁵
<i>Colwellia psychrerythraea</i> 34H	Putative lipoprotein	XP_001464756.1	3e ⁻⁵
<i>Beijerinckia indica</i> subsp. <i>indica</i> ATCC 9039	Protein of unknown function, DUF306 Meta and HslJ	YP_001832384.1	3e ⁻⁵
<i>Bacteroides vulgatus</i> ATCC 8482	Hypothetical protein BVU_2381	YP_001299662.1	5e ⁻⁵
<i>Hyphomonas neptunium</i> ATCC 15444	hypothetical protein HNE_0979	YP_759703.1	6e ⁻⁵
<i>Opiritaceae bacterium</i> TAV2	Heat shock protein-like protein	ZP_03723590.1	9e ⁻⁵

Phylogenetic relationship between META1 and HslJ

In order to study the phylogenetic linkage between META1 and HslJ, we generated a phylogenetic tree based on the protein sequences of META1 homologs in trypanosomatids and HslJ homologs in bacteria. A multiple sequence alignment containing 30 sequences (16 trypanosomatid and 14 bacterial) was used to create a phylogenetic tree using PhyML. Topology of the phylogenetic tree and the bootstrap values of the branch points (Figure 3), again indicate the occurrence of a LGT event of *META*/*hslJ* from bacteria to a trypanosomatid.

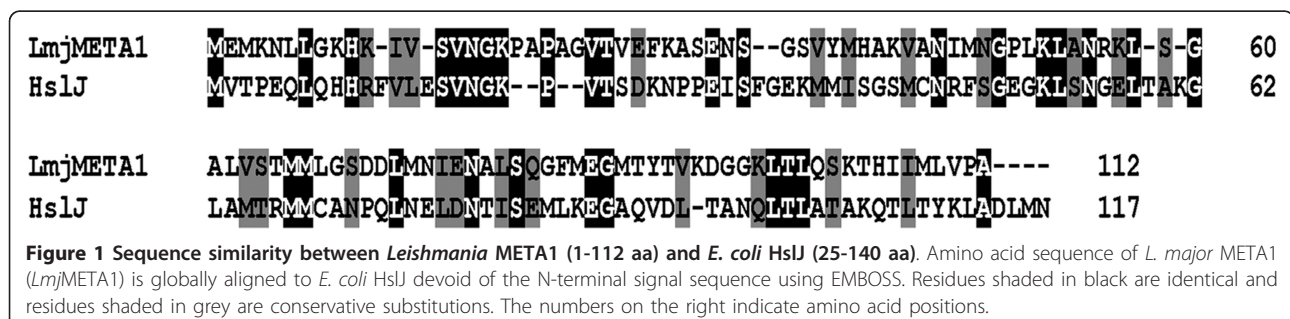
Synonymous and non-synonymous rate estimates

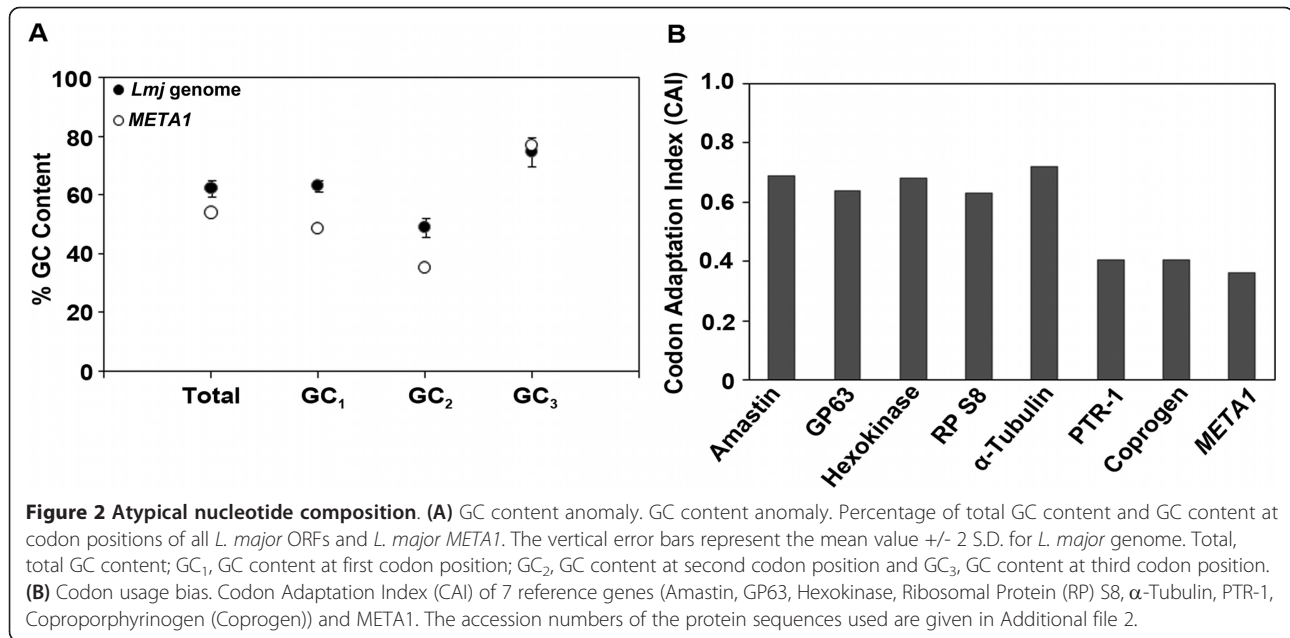
Estimation of synonymous (K_s) and non-synonymous substitution (K_a) rates is an important tool for understanding molecular sequence evolution and the ratio of

non-synonymous to synonymous rate of substitution (K_a/K_s) reflects the selection pressure on a gene [23]. We observed that *META1* and the META domain in bacterial *hslJ* homologs are under strong purifying selection as indicated by the K_a/K_s values < 1 in a pairwise comparison of *Lmj*META1 and META domain of 14 bacterial *hslJ* homologs (Figure 4). Therefore, lower substitution rates for *META1* emphasizes the selection pressure on it, a constraint on the *Leishmania* genome not to change it rapidly and thus, the importance of conservation of this gene.

META1 expression in *Leishmania*

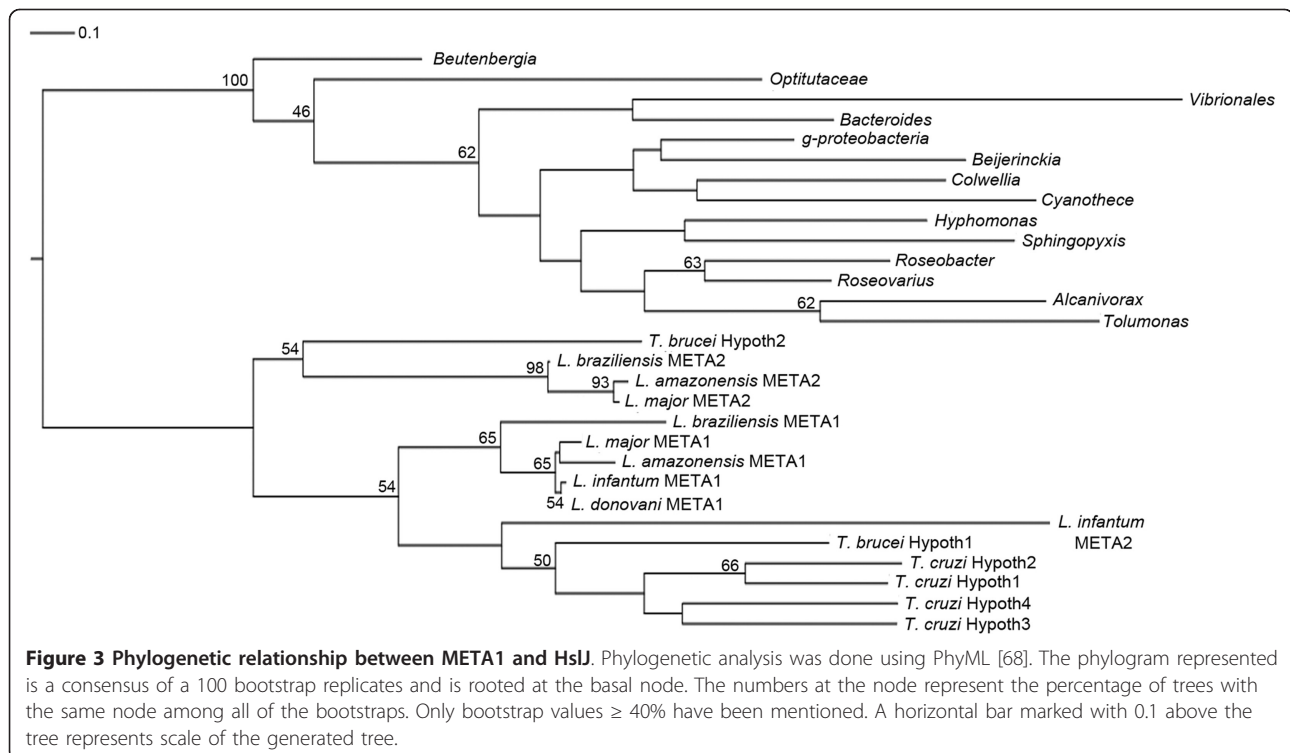
hslJ transcript is up-regulated in more pathogenic strains of *E. coli* [24] and the protein is heat inducible [25]. To delineate similarities between *META1* and *hslJ*,

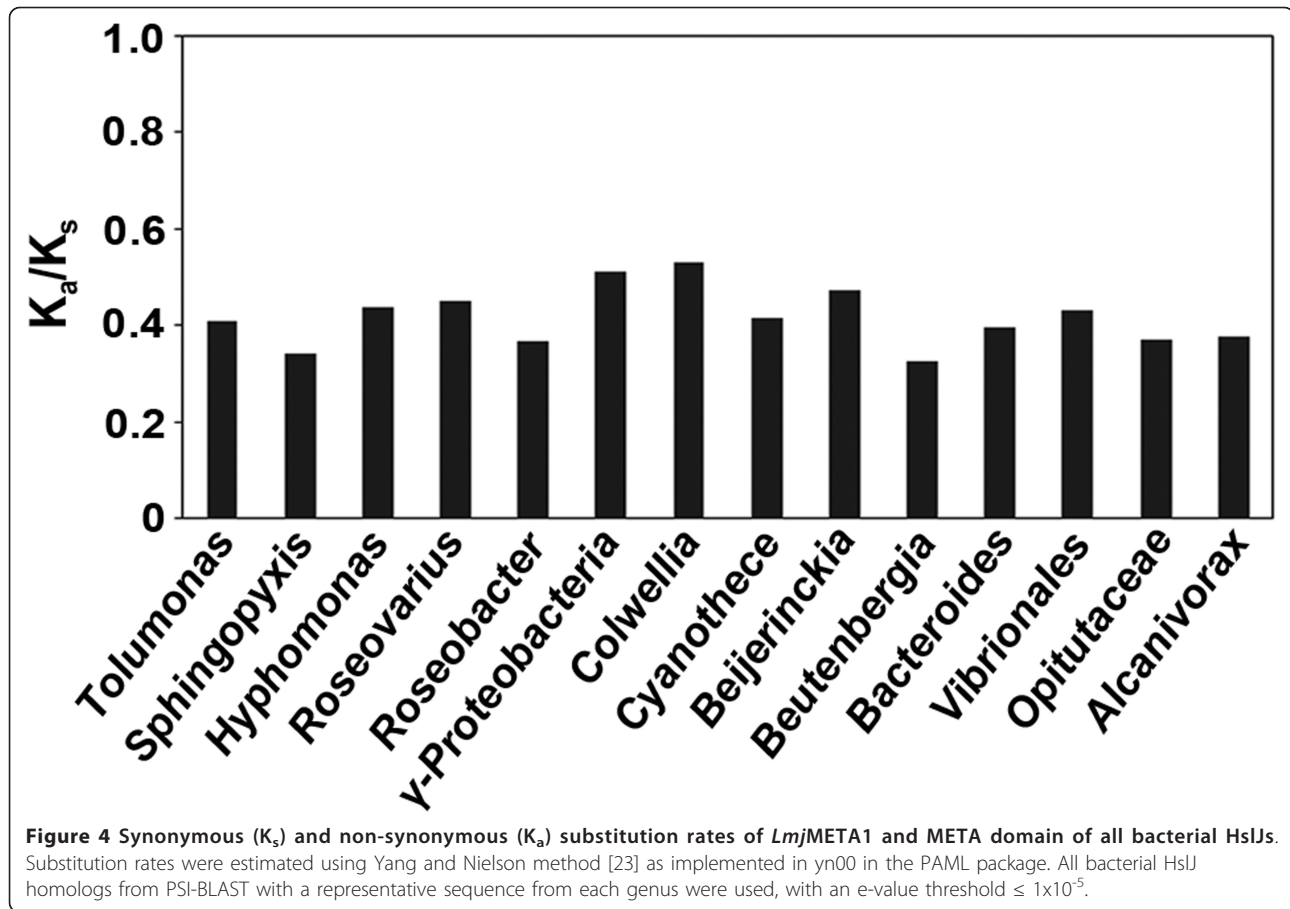




we investigated the expression pattern of *META1*. *META1* transcript levels were determined by QRT-PCR at different developmental stages of virulent and attenuated lines of *L. donovani*. *META1* transcript is up-regulated from log to stationary phase promastigotes as well as from promastigote to amastigote stage (Figure 5A).

META1 protein in *L. donovani* is maximally expressed in amastigotes (Figure 5B) even though *META1* transcript levels in amastigotes are lower than stationary phase promastigotes. *META1* protein is induced within 24 hours of shift to amastigote culture conditions, increases further upto 48 hours and its expression





decreases within 24 hours of reversal back to promastigote conditions (Figure 5C). The most striking observation is that attenuated *Leishmania* have reduced META1 expression under all conditions, as compared to virulent cells (Figure 5).

Acidic pH and increased temperature (shift from 26°C to 37°C) are very important cues for the *in vivo* as well as *in vitro* conversion of promastigotes to amastigotes [26-28]. Since we found that META1 is up-regulated in amastigotes stage, we investigated the role of these two parameters individually. We found that while both acidic pH and increased temperature induce META1 expression, increased temperature has a greater effect (Figure 5D). Levels of META1 on western blots have been quantified as shown in Additional file 4.

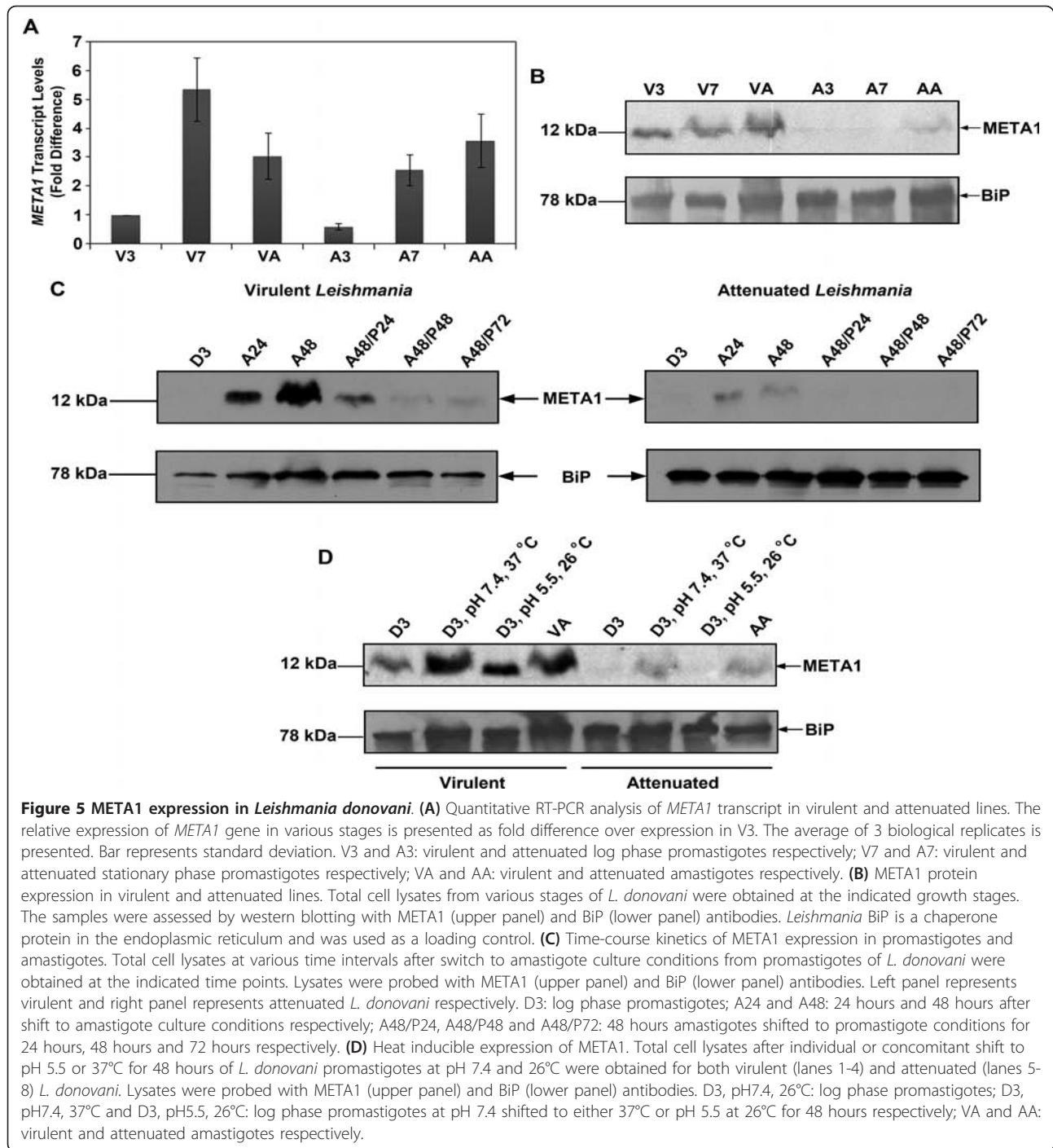
Structural homology between META1 and HslJ

In the absence of a solved structure of *Leishmania* META1 protein, we used 3D-JURY [29] structure prediction to look for structural homologs of META1. Consistent with our earlier searches, we found the top scoring model for META1 was based on *E. coli* HslJ. HslJ structure has 10 β -strands, which resembles a β -barrel structure except of the discontinuity caused due to the

presence of the α -helix. We also generated a structural model by homology modeling using MODELLER 9v2 [30] for *Leishmania* META1 using *E. coli* HslJ (PDB code 2kts) as the template. The final model (Figure 6A) comprises of complete META1 sequence (1-112) threaded on known NMR structure of *E. coli* HslJ (PDB code 2kts) for residues 25-140 (Figure 6B). The two proteins share a similar structural fold given that 107 C_α atoms of total 116 C_α atoms across the length of the proteins could be superposed with a root mean square deviation (RMSD) value of 1.2 Å and a sequence identity of ~ 28%. The striking structural similarity underscores that despite low sequence identity, META1 and HslJ have been under evolutionary constraints to retain a similar fold.

Comparison to proteins with similar folds of known function

Since little is known about *E. coli* HslJ's function with respect to its structure, we decided to look for additional proteins with similar fold. In DALI server [31], we found a structural homolog of HslJ: the *Shigella flexneri* protein MxiM (Figure 6A and Additional file 5). Despite a low sequence identity between HslJ and MxiM of only ~13%, 94 C_α atoms of the total 116 C_α atoms could be



superposed with an RMSD value of 2.5 Å, as determined by DALI pairwise comparison [32]. Similarly, *META1* and *MxiM* share a sequence identity of ~9%; yet, 94 C_α atoms out of the total 115 C_α atoms could be superposed with an RMSD of 2.6 Å. *MxiM* is a type III secretion apparatus (TTSS) pilot protein, which is a 142-residue lipoprotein, essential for the assembly and membrane association of the *Shigella* secretin, *MxiD* [33]. A deficiency in *MxiM*

leads to complete loss of TTSS function and virulence [34]. The structure of *MxiM* contains a 'cracked barrel' motif that creates a striking cleft in the centre of the protein. The cavity is entirely hydrophobic in nature and binds to lipid moieties of outer membrane (OM) of the bacteria [35]. Likewise, we observed that *META1* and *HslJ* also have a similar hydrophobic cavity upon their superposition to *MxiM* (Figure 6C). However, unlike in *MxiM*, the

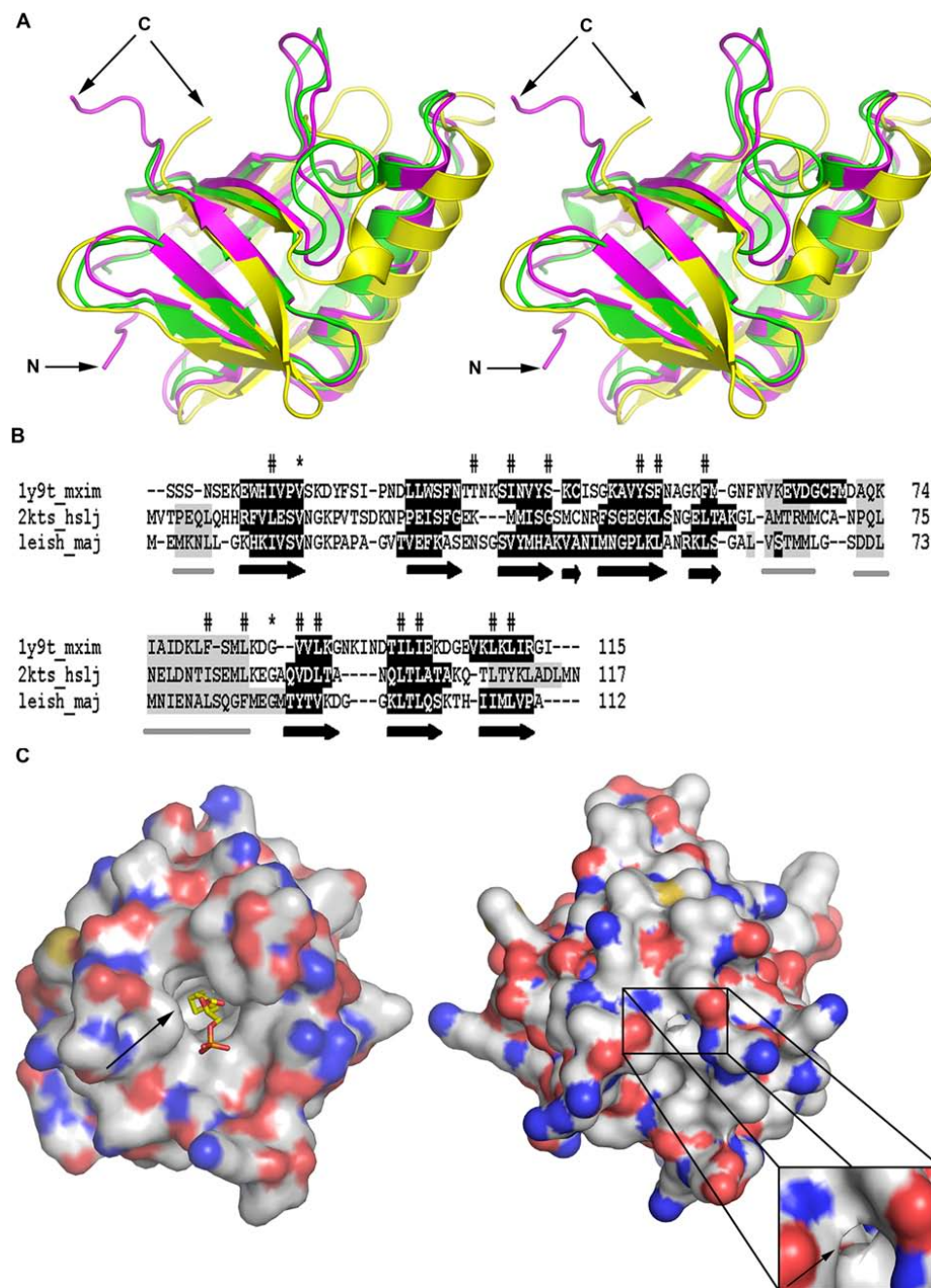


Figure 6 Structural similarities between META1, HsJ and MxiM. (A) Superposition of META1 (green), HsJ (magenta; PDB code 2kts) and MxiM (yellow; PDB code 1y9t) in stereoscopic view. The arrowheads mark the N-terminus and the C-terminus of the proteins. The figure was prepared using the software PyMol [73]. (B) META1 and HsJ sequence alignment based on MxiM structural superposition. Regions marked by horizontal grey bars below the alignment indicate helices and its corresponding amino acids are also shaded in grey. Beta strands are marked by black bold arrows below the alignment and the corresponding amino acid residues are shaded in black. Conserved residues are marked by (*) above the alignment. Amino acid residues lining the core of the hydrophobic cavity deduced based on structural superposition of META1 and HsJ with already described pocket of MxiM, are marked by (#). The alignment was generated by PROMALS3D [63]. (C) Molecular surface representation of MxiM (1y9t, left panel) and *Leishmania* META1 (right panel) highlighting their respective hydrophobic cavities. This representation was generated by superposing *Leishmania* META1 (right panel) onto MxiM (left panel, 1y9t) with its ligand in the proposed hydrophobic cavity. The surface is colored according to atom type: carbon atoms in grey, sulphur atoms in yellow, nitrogen atoms in blue and oxygen atoms in red. A zoom in view of the putative hydrophobic cavity of *Leishmania* META1 is represented as inset. Hydrophobic cavities of the both proteins have been indicated by an arrow. First 4 amino acids from the N-terminus from *Leishmania* META1 have been removed for clarity. The figure was prepared using the software PyMol [73].

putative hydrophobic cavity in META1 has at least one charged residue in its core (Figure 6B). Overall, structural comparisons between META1, HslJ and MxiM further reinforce their fold similarity. This pattern of structural and not sequence conservation signifies selection pressure on the structure of these proteins, probably for maintaining similar functions.

META1 is involved in secretory processes in *Leishmania*

In *L. major*, META1 is reported to localize around the flagellar pocket [16], the site for exo- and endocytosis in *Leishmania* [36]. MxiM, in addition to its known participation in *Shigella* TTSS, is also known to be structurally similar to the bacterial lipocalin [35]. Lipocalins are known extracellular transporters that bind small hydrophobic molecules [37]. Against this background of information, the striking structural similarity between META1 and MxiM prompted us to examine whether *Leishmania* META1 had a role in *Leishmania* secretory processes. Secreted acid phosphatase (SAP) is the most abundant secreted glycoprotein of *L. donovani* [38-40] and estimation of extracellular SAP activity is routinely used as an indicator of the status of secretory processes in the parasite [41-43]. Therefore, SAP activity was assayed in culture supernatants in the context of different levels of META1. Extracellular SAP activity was found to be lower at both log and stationary phase in *L. donovani* virulent promastigotes that have more META1 protein, when compared to attenuated promastigotes (Figure 7). In order to determine whether extracellular SAP activity is directly related with levels of META1 expression, we ectopically expressed META1 in both virulent and attenuated *L. donovani* promastigotes. The ectopic copy of *L. donovani* META1 protein was tagged with GFP at the C-terminus to distinguish from the endogenous protein. On META1 overexpression, extracellular SAP activity further reduced in both virulent and attenuated overexpression lines in comparison to their respective wild-types (Figure 7). Overexpression of META1 at protein level and its effect on growth kinetics is shown in Additional file 6. This suggests that cells having higher amounts of META1 protein have lower extracellular SAP activity, indicating a role for META1 in secretory processes in *Leishmania*.

Mutations in putative hydrophobic cavity of META1 alter secretion in *Leishmania*

To examine whether the predicted hydrophobic cavity has any role in META1's function, we decided to mutate smaller hydrophobic residues in the cavity to bulkier ones, wherein we replaced leucines at 58th and 80th position with a phenylalanine individually and both simultaneously (L58F or/and L80F). L58 is located at the entry of the cavity and is conserved across

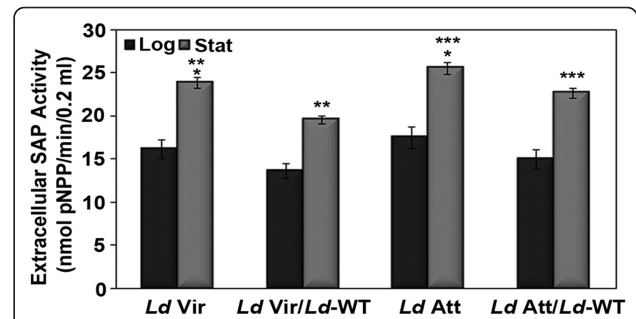
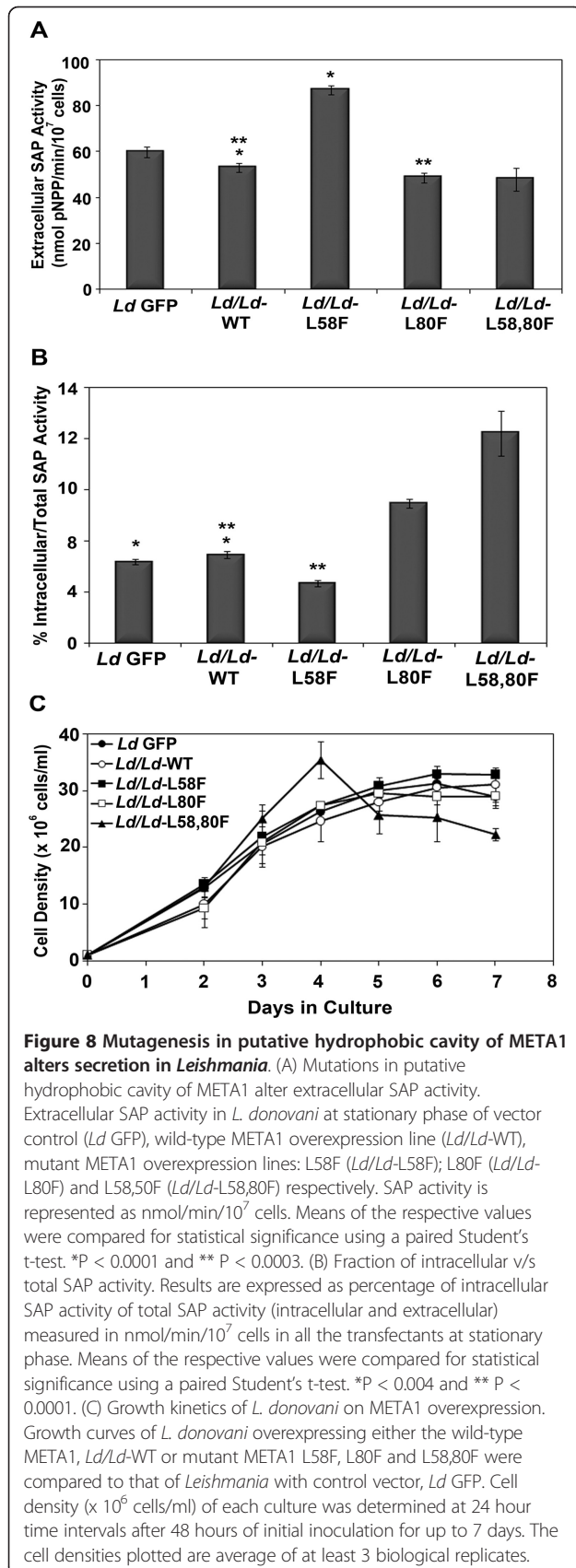


Figure 7 META1 is involved in secretion in *Leishmania*.

Extracellular SAP activity at log (black bars) and stationary phase (grey bars) of wild-type (*Ld Vir* & *Ld Att*) and META1 overexpressing (*Ld Vir/Ld-WT* & *Ld Att/Ld-WT*) *L. donovani* virulent & attenuated promastigotes lines respectively. SAP activity is represented in nmoles of pNPP hydrolyzed per min per 0.2 ml. The average of at least 5 biological replicates is presented. Bar represents the standard deviation. Means of the respective values at stationary phase were compared for statistical significance using a paired Student's t-test. *P < 0.005, **P ≤ 0.0002 and ***P ≤ 0.005.

trypanosomatids and bacterial HslJ. On the other hand, L80 is inside the hydrophobic cavity and is conserved in trypanosomatids, with the exception of *L. braziliensis* and *T. cruzi* as shown in Additional file 7. Mutant proteins were C-terminally tagged with GFP, in order to distinguish from endogenous protein and were ectopically expressed in *L. donovani* promastigotes.

Extracellular SAP activity increased by 40% in *L. donovani* overexpressing L58F mutant META1 protein, as compared to cells overexpressing the wild-type (WT) META1 (Figure 8A). However, L80F mutation in META1 decreased the extracellular SAP activity with respect to WT overexpression. Moreover, extracellular SAP activity of the double mutant L58,80F was found to be similar to that of L80F mutant in *L. donovani* (Figure 8A). We also determined the intracellular SAP activity in all of these *Leishmania* lines. Consistent with the changes in extracellular activity, the percentage of intracellular v/s total SAP activity is higher in cells overexpressing WT, L80F and L58,80F META1, but lower in the L58F mutant, as compared to GFP control (Figure 8B). These results suggest that the 58th and 80th position are critical for the function of META1 in *L. donovani*. Similar results were obtained when L58F and L80F mutations were introduced into *L. major* META1, either individually or simultaneously (Additional file 8), reiterating that the *L. donovani* and *L. major* META1 proteins have a conserved function. We also observed a growth defect only in the double mutant in both *L. donovani* and *L. major*, which have higher multiplication rate at late logarithmic phase and start declining sooner than WT overexpression cells (Figure 8C and Additional file 8 respectively). The difference in SAP activity



between cells overexpressing WT versus META1 mutant forms was not due to different amounts of META1 protein being expressed, as shown by western blots (Additional files 6 and 8). In order to eliminate the possibility of misreporting extracellular SAP activity due to cell lysis, a western blot on culture supernatants was done with GP63 and BiP antibodies, along with whole cell lysates as control. The culture supernatants that we used for the experiment did have extracellular GP63 but lacked ER chaperone BiP, as shown in Additional file 9. Overall, alteration in extracellular SAP activity in cells expressing META1 mutants points to a role for META1 in *Leishmania* secretory processes and highlights the importance of the putative hydrophobic pocket to META1's function.

Discussion

Despite *Leishmania* META1's well known association with virulence, its functions have remained poorly understood. We have attempted to elucidate the functions of META1 by identifying and examining its known homologs in other organisms. We have observed an unusual phyletic relationship between bacterial HslJ and trypanosomatid META1 which highlights LGT as the most rational explanation for the origin of META1 sequences in trypanosomatids.

Analyses of several pathogen genomes suggest a widespread occurrence of LGT [20,22,44-49]. These studies have relied on combinations of aberrant nucleotide composition or sequence similarity searches and phylogenetic analyses. In our study we have included all of these approaches: sequence similarity, overall GC content bias, GC content bias at 1st and 3rd codon positions and codon usage bias of META1 over whole genome of *L. major* and phylogenetic distribution pattern. All of the individual analyses are consistent with the notion of META1 being laterally transferred from bacteria into trypanosomatids (Figures 2 and 3). In the analyses of such LGT events it is crucial to factor in multiple lines of evidence [50]. By itself, the phylogenetic tree may be open to additional interpretations such as a "reverse" LGT flow from trypanosomatids into bacteria or a retention of META1 in trypanosomatids, from a common ancestor (with bacteria) with a loss from other species. However, the consistent topology of the phylogenetic tree, rooted in multiple manners (Figure 3 and Additional file 10) taken together with the striking anomalous nucleotide composition of META1 in *Leishmania* make it unlikely that the LGT flow of META1 was from trypanosomatids into bacteria. Or, that META1 was retained within *Leishmania* from a common ancestor: if META was persisting from an ancient common ancestor, its GC composition would have been assimilated into the trypanosomatid genomes. However, we cannot exclude a possibility that META1

was present in an ancient common ancestor, was lost during the evolutionary emergence of eukaryotes and at some point, regained by trypanosomatids through a LGT from bacteria. Clearly, more definitive answers to such events will emerge as the genome sequence information coverage of various taxa expands.

Analyses of anomalous nucleotide composition is quite effective in the detection of recent LGT events but becomes handicapped as the time scale of the event in question increases typically because the gene in question has more time to adjust to the host genome [50]. Given the diversity of bacterial species that have the META domain and the limited occurrence of META only in trypanosomatid eukaryotes, it is most likely that the transfer of META1 into trypanosomatids was an ancient event. In this regard, it is striking that the anomalous nucleotide composition of *Leishmania* META1 continues to be easily discernible.

Maintenance of the foreignness of a laterally transferred gene in the context of its recipient genome could reflect either a recent transfer event or a selective pressure to maintain certain features. Given the occurrence and conservation of *META1* sequence throughout trypanosomatids, it is most likely the transfer of META1 from bacteria was an early event into a trypanosomatid ancestor. An organism always maintains certain evolutionary constraints on its essential genes, in order to prevent loss of function caused due to mutations. Thus, a gene under purifying selection will evolve at a slower rate than a gene under positive selection. Upon comparison of *META1* with its bacterial homologs, we found that *META1* is under strong purifying selection, therefore, highlighting the importance of function of this gene for the organism (Figure 4).

Selection constraints on the META1/HslJ pair also underline the possibility of having similar properties. Our results have highlighted some of the properties shared by HslJ and META1. *hslJ* transcript up-regulation was found to be associated with pathogenicity in *E. coli* [24] and recovery of heat injured *Salmonella enteritidis* [51]. In comparison, we observed that *META1* expression too is regulated in developmental stages in *L. donovani*, consistent with earlier reports [17]. We have also shown that attenuated *Leishmania* have lower META1 expression than virulent cells, consistent with a role for META1 in *Leishmania* virulence. In *Leishmania*, META1 expression is inducible by both temperature and acidification, with the temperature-mediated change being more significant (Figure 5). This observation underscores the heat-inducible property of META1, like its bacterial homolog HslJ [25].

HslJ has been associated with increased resistance against a gyrase inhibitor novobiocin [52]. We examined in *Leishmania* if META1 expression is associated with

novobiocin resistance in virulent & attenuated lines of *Leishmania* as well as in META1 overexpressing lines. In the above mentioned conditions, we found no such correlation (data not shown). Clearly, not all functions are common between META1 and HslJ. Recently, *L. amazonensis* META2 that has 3 META domains and a C-terminal calpain-like domain was reported to be implicated in novobiocin resistance [53]. This raises the possibility that our observations may be explained by META2 complementing for novobiocin resistance independent of META1 expression levels.

The 3D-modeling studies of META1 allowed us to identify an additional structural homolog of META1, the secretin pilot protein of *Shigella flexneri*, MxiM (Figure 6A). These three proteins: META1, HslJ and MxiM share a strikingly similar fold, in spite of a very low sequence identity. The essential features about the structural similarity of these proteins highlighted upon superposition are: a common cracked barrel motif and a set of conserved hydrophobic residues in the central pocket of the protein (Figure 6B). Such a structural homology between META1, HslJ and MxiM suggests a possibility of similar function of these proteins. Many proteins with similar function have been known to retain similar structural folds despite very low sequence identity and ambiguous secondary structure prediction [54,55]. The hydrophobic cavity in MxiM is known to bind lipid moieties of bacterial membranes. However, unlike MxiM, the putative cavity of META1 has at least one charged amino acid suggesting that the ligand of this putative pocket may be different from MxiM (Figure 6B). It is possible that these proteins participate in similar activities, with certain residues in the cavity defining specificity of the ligand.

Changes in levels and predicted structure of META1 affect the quantum of extracellular activity of the well characterized marker for *Leishmania* secretory processes, SAP (Figures 7 and 8). A comparison of proportion of intracellular v/s total SAP activity shows that overexpression of either WT or mutant META1 changes the extracellular SAP secretion (Figure 8B). However, while ectopic expression of L80F mutant and WT reduces extracellular SAP activity, the L58F mutant META1 caused an increase in extracellular SAP activity. The L58F mutation appears to act as a loss of function event: there is more META1 protein but with a reduced negative effect on SAP activity. The proximity of this 58th position to the entrance of the putative hydrophobic cavity (Additional file 7) suggests impairment in interactions with the probable ligand of the putative cavity that may interfere with META1's function, in turn interfering with META1's ability to suppress SAP secretion. Additionally, in *L. donovani*, L58 epitopic region seems to be highly antigenic: when lysates of cells overexpressing the different forms of META1 were probed with polyclonal

META1 antisera on a western blot, the L58F reactivity was extremely low compared to WT overexpression control. However, when the same proteins, all of which have GFP tagged to their C-termini, were probed with polyclonal GFP antibody, cell lysates exhibited equivalent amounts of GFP-tagged proteins (Additional file 6).

The L80F mutation dominates over L58F mutation in case of the double mutant (L58,80F), as seen by its overall effect on SAP activity (Figures 8A and 8B). Contrary to the L58 position, L80 lies in the core of the cavity: this change in position may also explain the altered consequences of the two mutations. Overall, our results on META1 mutagenesis in its putative hydrophobic cavity are consistent with a role for META1 in secretory processes in *Leishmania* and that this cavity is important for META1's function. However, the double mutant has an altered growth (Figure 8C), suggesting that META1 may also be participating in events other than secretion.

Overall, the consequences of META1 mutations on extracellular SAP activity are consistent in both *L. donovani* and *L. major*: L58F overexpression leads to increased SAP activity; L80F has an equivalent effect on SAP activity to WT META1 and L80F dominates over L58F in the double mutants (Additional file 8). Additionally, the L58F,80F double mutant has growth effects in both species (Figure 8C and Additional file 8). However, we did observe some differences between the two *Leishmania* species. One, the extent of effect on SAP activity is greater in *L. donovani*. Second, L80F has distinct effects in *L. major*. In *L. major*, L80F and L58,80F mutant META1 protein expression was not seen while L58F mutant protein is equivalent in expression as the overexpressed WT (Additional file 8). In spite of the presence of *META1-GFP* fusion transcripts in both L80F and L58,80F (Additional file 8), there is barely any detectable amount of mutant protein suggesting that the mutant protein is possibly getting degraded. These observations reiterate the fact that L80F mutation is dominant in L58,80F mutation. Since L80 lies in the core of the cavity which might be important for ligand binding (Additional file 7), it is possible that mutation at this site has disrupted ligand binding resulting in an unstable META1 conformation, leading to its degradation.

It is increasingly clear that LGT is an important mechanism in the evolution of eukaryotes [50,56]. An interesting finding has been the observed transfer of gene sets for metabolic pathways [22,57]. This is particularly of importance in the case of unicellular eukaryotes: LGT from bacteria allows the acquisition of new abilities such as exploitation of ecological niches, infective abilities and metabolic capabilities. A practical advantage of such knowledge is that such LGT acquired genes are more likely to be conducive targets for drug development since the host eukaryote typically lacks these genes [50,57].

Furthermore, over time, LGT event has played a significant role in the subsequent evolution of the *META1* gene family in trypanosomatids, as can be seen from the occurrence of a number of paralogs in Trypanosomes and a separate gene in *Leishmania*, *META2*, which has three META domains.

It is conceivable that, for *Leishmania*, at least one of the advantages of the LGT mediated acquisition of META1 was additional modulation of secretory processes. Secretion can be an important process for a pathogen seeking to modulate its host's responses via the export of effector molecules/virulence factors. *Leishmania* secrete various bioactive molecules that are involved in pathogenesis [58]. Recently, a novel exosome-based pathway was identified as a general mechanism of protein secretion by *Leishmania* that is involved in pathogen-to-host communication and export of exosomal cargo into host macrophages [59]. Furthermore, the exosomal cargo influences myeloid cells and is immunosuppressive [60]. Our data is consistent with the correlation of META1 levels associated with *Leishmania* virulence. This work adds new information on functional role for META1 in secretory processes in *Leishmania*. Additionally, it identifies a domain within META1 that may be critical for its functions.

Conclusions

META1 has long been associated with virulence but its activity and the processes it influences to modulate virulence have remained unknown. In order to identify the function of this enigmatic yet essential protein, we have used an evolutionary biology approach to first identify the origins of META1. Having provided several lines of evidence that *META1* arose in *Leishmania* as the result of a LGT event of *hslJ* from bacteria, we leveraged this information to get clues about META1 function by comparing it to its bacterial homologs. We utilized 3D-modeling to show that META1 shares a structural scaffold with HslJ and MxiM. The striking structural similarity between these proteins despite a limited sequence homology points to evolutionary constraint on retaining structural folds in proteins and the retention of related functions. The sequence divergence most likely allows for specificity of interacting molecules. The conserved scaffold between META1/HslJ/MxiM identified a shared cavity in these proteins. We have extended the known involvement of MxiM in secretion and the possibility of a role for such a cavity with regards to META1 function. Using molecular biology approaches, we demonstrate that ectopic expression of META1 and site-directed mutagenesis of selected residues in the predicted META1 cavity do affect secretory processes in *Leishmania*, thus establishing a function for this poorly characterized protein as well as identifying a functional domain within the molecule. Overall, our study demonstrates the utility of a multidisciplinary approach

that combines insights from evolutionary origins of a molecule with bioinformatics analyses and computational approaches, leading to a predicted structure and activity, both of which are testable at a molecular level.

Methods

Sequences, sequence similarity searches and sequence alignment

BLASTP and PSI-BLAST searches [61] were performed against the NRDB using the NCBI server <http://www.ncbi.nlm.nih.gov/BLAST>. Pfam search [62] was performed using HMMer via the Pfam server at <http://pfam.sanger.ac.uk/>. All the sequences (DNA/protein) used in the study for codon bias, phylogenetic analysis and synonymous & non-synonymous rate estimation were obtained from NCBI. For *E. coli* HslJ, sequence information was used from accession number NP_415897.1. Sequence alignment was done with CLUSTALW available at <http://www.ebi.ac.uk/clustalw/> or EMBOSS <http://www.ebi.ac.uk/Tools/emboss/align/index.html>. Sequence to structure alignment was done with PROMALS3D software available at <http://prodata.swmed.edu/promals3d/promals3d.php> [63].

GC content

Total GC content and GC content at codon positions for all *L. major* ORFs and *META1* was obtained using Integrated Genomic Island Prediction Tool (IGIPT) software available at <http://ccnsb.iit.ac.in/nita/IGIPT/srk/index.php> [64]. FASTA files for all *L. major* ORFs was obtained from the Wellcome Trust Sanger Institute at ftp://ftp.sanger.ac.uk/pub/databases/L.major_sequences/.

Codon usage bias

For calculating Codon Adaptation Index (CAI), the Relative Synonymous Codon Usage (RSCU) values of the highly expressed genes of *L. major* were obtained from [65]. CAI values of reference genes from Additional file 2 and *META1* were calculated manually as described earlier [66].

Phylogenetic analysis

The sequences were aligned using MUSCLE [67] on default settings. Gaps were removed from the alignment manually. Phylogenetic tree was generated by PhyML [68] using the evolutionary model WAG, the gamma-distribution model, four rate categories and invariant position. The WAG model was found to be the best-fitting model using PROTTEST [69]. The gamma parameter and the fraction of invariant positions were estimated from the data. The trees were optimized for topology, branch length and rate parameters. Each tree was subjected to 100 bootstrap replicates. iTOL [70] was used for viewing the phylogenetic tree and later on modified in

Adobe Photoshop CS4 for publication. Re-rooting of the tree was also done using iTOL. The accession numbers of the protein sequences used are given in Additional file 11.

Estimation of substitution rates

Synonymous (K_s) and non-synonymous (K_a) substitution rates were estimated using the methods as described earlier [23] as implemented in yn00 in the PAML software [71].

Molecular modeling of *Leishmania* META1

Consensus structure prediction for META1 was performed using 3D-Jury <http://bioinfo.pl/meta>; [29]). MODELLER 9v2 [30] software was used to obtain the final model of META1 based on the NMR structure of an *E. coli* HslJ (PDB code 2kts). The model was viewed using the program O [72] and was compared with that of the template and related structures. The program O was also used for superposition of META1 and HslJ structures on that of *S. flexneri* secretin pilot protein, MxiM (PDB code 1y9t) for comparison. The figures were made using PyMol [73].

Leishmania strains and growth condition

L. donovani MHOM/IN/1983/AG83 and *L. major* MHOM/Su73/5ASKH were used for all the experiments. The conditions for promastigotes *Leishmania* cultures are as described earlier [74]. For all experiments, cell numbers were estimated by direct counting in a hemocytometer under a light microscope. The promastigotes were routinely inoculated at a starting density of 10^6 cells/ml; typically, logarithmic growth was observed between day 2-4 and stationary phase between day 5 and 7. Hence, in all experiments, 3 days and 7 days old cultures were used as representative of log phase and stationary phase respectively. For axenic amastigotes, log phase promastigotes were pelleted down by centrifugation at 3000 rpm for 10 min, washed with PBS and resuspended in amastigote media (Complete HOMEM, 20% FCS, pH 5.5) and incubated at 37°C with 5% CO₂ for 48 hrs. Promastigotes convert into amastigotes within 48 hrs. For generating attenuated parasite line, virulent promastigotes were passaged in HOMEM medium once a week until 30 passages and thereafter, infectivity of the parasites were checked in BALB/c mice after 4 weeks of inoculation.

RNA isolation, reverse transcription and quantitative real time (QRT) PCR analysis

Total RNA was isolated using the acid guanidinium isothiocyanate method [75]. 1 µg of total RNA from *L. donovani* was treated with DNase I (Ambion Inc.). Synthesis of cDNA was performed by using First Strand

Synthesis kit and the Superscript III Reverse Transcriptase (Invitrogen), according to the manufacturer's instructions. All real-time PCR experiments were performed in ABI prism 7900 HT sequence detection system (ABI) as described earlier [76]. The PCR conditions were as follows: 95°C for 10 min, 95°C for 15 sec, 58°C for 30 sec and 72°C for 30 sec for 40 cycles. Following primers were used in QRT-PCR analysis; for *LdMETA1*: TV359 & TV360, for *LmjMETA1*: TV672 & TV758, for neomycin: TV 397 & TV398, for GFP: TV276 & TV396 and for *GAPDH*: TV366 & TV367. Sequences of all the primers are mentioned in Additional file 12. All the reactions were analyzed using the software (SDS 2.3) provided with the instrument. The relative expression of the genes was calculated by using $2^{-\Delta\Delta C_t}$ formula using *GAPDH* as a normalizer. The values reported are the mean of at least three biological replicates. The standard deviation from the mean is shown as error bars in each group.

Expression and purification of recombinant *LdMETA1* protein and generation of antibodies

The *LdMETA1* coding region was PCR amplified from *L. donovani* genomic DNA, using primers TV213 & TV215 and cloned in *EcoRI-HindIII* site of pET28a+ vector (Novagen). Primer sequences are listed in Additional file 12. The recombinant constructs were transformed in *E. coli* BL21 (DE3) strain and protein expression was induced at A₆₀₀ of 0.6 with 1 mM of isopropyl-1-β-D-galactopyranoside at 37 °C for 3 hours. Recombinant 6X-His-META1 protein was purified from bacterial cells in native conditions using the Ni²⁺-nitrilo triacetic acid agarose resin (Qiagen), according to the manufacturer's instructions.

For raising polyclonal antibodies against recombinant 6X-His-META1 protein in the mouse, 50 µg/animal of protein was mixed with an equal volume of Freund's complete adjuvant. The mixture was made into an emulsion by passing through a 2 ml syringe (1.5 inch 19G needle) and intermittently keeping it at 4°C. This emulsion was injected into the mouse subcutaneously. After 14 days, the first booster dose was given in a similar manner, except that Freund's complete adjuvant was replaced with Freund's incomplete adjuvant. Subsequent booster doses were given after a 14-day interval and the antibody titer was checked using dot blot. For determination of antibody titer 20 ng of purified protein was spotted in a row, air-dried and incubated with different concentrations of immune serum (1:1,000 to 1:5,000). Western blot experiments were carried out when the appropriate titer (1:5,000) was obtained following booster doses. Mice were sacrificed and blood collected from the inferior vena cava using a 23G needle and a 2 ml syringe. The blood was

allowed to stand at room temperature for a couple of hours and then kept at 4°C for overnight to allow formation of a firm clot. Red blood cells were removed by centrifugation, the sera were collected in a fresh tube, 0.2% NaN₃ was added and stored at 4°C. All experiments involving animals were performed in compliance with recommendations and permission of the CCMB Institutional Animal Ethics Committee.

Generation of pX63-META1::GFP constructs

The *META1* gene of both *L. donovani* and *L. major* were cloned in frame with *GFP* at the C-terminus and further this *META1-GFP* cassette was ligated into *BamHI-XbaI* site of pX63-NEO vector. The *L. donovani* and *L. major META1* genes were amplified from genomic DNA by using the primer combinations TV494 & TV757 and TV494 & TV758 respectively and *GFP* was amplified using TV276 & TV277 from pX63-EGFP vector. PCR amplicons of *META1* gene of both *L. donovani* & *L. major* and *GFP* were first cloned using pMOS blunt end cloning vector kit (GE Healthcare) as per manufacturer's instructions. Inserts were released from pMOS by using restriction enzymes inserted in the primer sequences. Extra sequences were added in the primers to maintain the reading frame and/or to add restriction sites for cloning: for *META1*, TV494 with a *BamHI* and TV757 & TV758 with *NcoI* site respectively and for *GFP*, TV276 & TV277 with an *NcoI* and *XbaI* site respectively. Primer sequences are listed in Additional file 12.

Transfection of plasmids into *Leishmania* promastigotes

Leishmania promastigotes were grown to late log phase (~2 × 10⁷ cells/ml). Transfection protocol is the same as described earlier [77]. Briefly, cells were washed and resuspended in ice cold electroporation buffer (137 mM NaCl, 5 mM KCl, 0.7 mM Na₂HPO₄, 6 mM glucose, 21 mM HEPES pH 7.5) at a density of 10⁸ cells/ml. 400 µl of cells and 100 µg of plasmid DNA were mixed well into 0.2 mm cuvettes (Biorad) then electroporated in Genepulser II apparatus (Bio-Rad Laboratories) with the pulse of 450 volts (2.25 V/cm) and capacitance 500 µF. Cuvettes were immediately placed on ice for 10 minutes. Cells were transferred to 5 ml of complete HOMEM media. After 48 hours, transformants were selected in HOMEM containing G418 until the control, untransfected cells died completely in the presence of the antibiotic. Concentrations of G418 used were: 40 µg/ml for virulent *L. donovani* & *L. major* promastigotes and 200 µg/ml for attenuated *L. donovani* promastigotes. For further experiments, pool populations were maintained in liquid media containing G418 in above mentioned concentrations for the respective cell types.

Site-directed mutagenesis

For generating constructs with point mutations in *META1*, site-directed mutagenesis (SDM) was carried out using QuickChange-XL kit from Stratagene as per manufacturer's instructions. pX63-*LdMETA1::GFP* (*Ld/Ld*-WT) and pX63-*LmjMETA1::GFP* (*Lmj/Lmj*-WT) were used as templates for SDM of *L. donovani* and *L. major META1* mutagenesis. Details of the primers used are given in Additional file 12.

Western blot analysis

Leishmania promastigotes or amastigotes at different stages of growth were harvested, washed in PBS and then resuspended in 1X-PBS with 1X-protease inhibitor cocktail (Roche) and then sonicated using VibraCell (Sonics & Materials Inc.) with 50% amplitude and three pulses for 30 sec each. 30 µg of protein lysate from each sample were separated on 15% SDS-PAGE and transferred onto nitrocellulose Hybond ECL membranes (Amersham Biosciences). Membranes were blocked with 5% non-fat dried milk in 1X-TBS-T (10 mM Tris-HCl, pH 8.0, 150 mM NaCl, 0.1% Tween-20). The following antibodies were used: mouse anti-*LdMETA1* (1:5,000) was raised against recombinant N-terminally 6X-His tagged *LdMETA1* protein, rabbit polyclonal BiP antisera (1:15,000), rabbit polyclonal GFP antibody (Abcam; 1:4000), sheep polyclonal GP63 antisera (1:10,000), anti-mouse or anti rabbit biotinylated antibodies (1:5,000, Amersham), avidin conjugated with horseradish peroxidase (1:10,000, Amersham Biosciences) and anti-sheep conjugated with horseradish peroxidase (1:5,000, Santa Cruz Biotechnology). After incubation, membranes were washed three times with 1X-TBS-T. Immunodetection was carried out using the ECL western blotting detection system (GE Healthcare) according to the manufacturer's instructions and images were obtained using BIOMAX™-XBT X-ray film (Kodak). Images of western blots were quantified by ImageJ software available at <http://rsbweb.nih.gov/ij/>[78].

For western blots on the culture supernatants, media from cultures were passed through a 0.22 µm membrane and concentrated 50-fold using Millipore Amicon 5 kDa cut-off and loaded onto SDS-PAGE gel along with whole cell lysates as control.

Secreted acid phosphatase (SAP) assay

SAP activity was determined in culture supernatants as previously described [41]. After seeding cells at a density of 10⁶ cells/ml, aliquots of culture medium were removed at log and stationary phase, filtered through 0.22 µm pores membrane to remove cells and debris. 138 µl supernatant was then incubated in a final volume of 200 µl with 50 mM para-nitrophenyl phosphate (pNPP), 50 mM sodium acetate pH 4 and 0.1% β-mercaptoethanol (v/v) for 30 minutes at 37 °C. The reaction was

stopped with 800 µl of 2M sodium hydroxide and the absorbance of the released para-nitrophenol was determined at 410 nm. For intracellular SAP activity, cell pellets were washed with PBS and were lysed on ice for 30 min at 10⁸ cells/ml in 50 mM acetate buffer and 1% Triton X-100. 100 µl of lysate was then used for SAP assay with 50 mM pNPP.

Additional material

Additional file 1: List of protein sequences obtained from BLASTP sequence similarity search for *LmjMETA1* against non-redundant NCBI database. Table S1. Description of BLASTP hits with their e-value.

Additional file 2: List of reference genes for CAI determination. Table S2. Description of reference genes used for CAI determination.

Additional file 3: Codon Adaptation Index (CAI) of *META1* homologs in *T. cruzi*. Figure S1. CAI of 2 *META1* homologs in *T. cruzi* compared with RP S8 and α-Tubulin.

Additional file 4: Quantitation of signal in western blots in Figure 5. Figure S2. Images of western blots in Figure 5B, C and 5D were quantitated by ImageJ software.

Additional file 5: Movie of superposed structures of HsIJ (magenta), MxiM (yellow) and *META1* model (green). Figure S3.

Additional file 6: Overexpression of *META1* in *L. donovani*. Figure S4. Western blots (S4A and S4B) of *L. donovani* virulent and attenuated *META1* transfectants with *META1*, BiP and GFP antibodies. S4C represents effect of *META1* overexpression on growth kinetics of virulent and attenuated *L. donovani* compared to their respective wild-types.

Additional file 7: Mutagenesis of *META1*. Figure S5. Sequence alignment of *META1* homologs and stereoscopic representation of *META1* model highlighting the leucine 58 and leucine 80.

Additional file 8: Effect of *META1* overexpression in *L. major*. Figure S6. Effect of WT and mutant *META1* overexpression in *L. major* on extracellular SAP activity (S6A) and growth kinetics (S6B). S6C and S6D represents western blot and QRT-PCR of *L. major META1* transfectants respectively.

Additional file 9: Western blot of *L. donovani* whole cell lysates v/s culture supernatants. Figure S7. Western blot with GP63 and BiP on whole cell lysates and culture supernatants of *L. donovani META1* transfectants.

Additional file 10: Phylogenetic tree re-rooted at two different roots. Figure S8. Phylogenetic tree representation generated in Figure 3 was re-rooted at *Tolomonas* (S8A) and *T. cruzi* Hypoth3 (S8B).

Additional file 11: List of protein sequences used in phylogenetic analysis. Table S3. Accession numbers of protein sequences.

Additional file 12: Primers used in the study. Table S4. List of sequences of all the primers used in this study.

Acknowledgements

We thank members of the Vaidya lab for useful discussions and suggestions. We thank Dr Steven M. Beverley for the pX63 plasmids, Dr Mary E. Wilson for GP63 antibody and Dr Jay Bangs for BiP antibody. We are grateful to Dr Nita Parekh and Ms Ruchi Jain from IIIT, Hyderabad, India for helping us with IGIPT software. We are thankful to Dr Harpreet K. Saini from EMBL-EBI for technical support and valuable suggestions. We thank Mr Aridaman Pandit from CCMB, India for helping us with phylogenetic tree construction. VP and AG were supported by senior research fellowships from CSIR, Government of India. VP was a recipient of 2007 Sanger Institute Prize and is grateful to the Wellcome Trust Sanger Centre Prize Fund (Grant number 079643/Z/06/Z) for financial support provided for research carried out at the Sanger Centre in AJE's lab and for supporting the cost of publication. This research was supported by the CSIR, Government of India to TV. Funding agencies have

no role in study design, data collection, analysis and writing of the manuscript.

Author details

¹Centre for Cellular and Molecular Biology, Council for Scientific and Industrial Research, Uppal Road, Hyderabad - 500 007, Andhra Pradesh, India. ²EMBL-EBI, Wellcome Trust Genome Campus, Hinxton, Cambridge, CB10 1SD, UK. ³Syngene International Limited, Biocon Park, Plot No. 2 & 3, Bommasandra Industrial Area-IV Phase, Bommasandra-Jigani Link Road, Bengaluru- 560099, Karnataka, India.

Authors' contributions

VP participated in design of the study, carried out bioinformatics analysis, laboratory experiments, analyzed the data and drafted the manuscript. AG and RS constructed the homology model and analyzed the structures. AJE helped design the analysis of evolutionary origin of META1, participated in data analysis and critically read the manuscript. TV participated in design of the study, supervised the work, analyzed the data and drafted the manuscript. All authors read and approved the final manuscript.

Competing interests

The authors declare that they have no competing interests.

Received: 19 September 2011 Accepted: 17 November 2011

Published: 17 November 2011

References

1. Brittingham A, Morrison CJ, McMaster WR, McGwire BS, Chang KP, Mosser DM: **Role of the *Leishmania* surface protease gp63 in complement fixation, cell adhesion, and resistance to complement-mediated lysis.** *J Immunol* 1995, **155**:3102-3111.
2. Chakrabarty R, Mukherjee S, Lu HG, McGwire BS, Chang KP, Basu MK: **Kinetics of entry of virulent and avirulent strains of *Leishmania donovani* into macrophages: a possible role of virulence molecules (gp63 and LPG).** *J Parasitol* 1996, **82**:632-635.
3. Joshi PB, Kelly BL, Kamhawi S, Sacks DL, McMaster WR: **Targeted gene deletion in *Leishmania major* identifies leishmanolysin (GP63) as a virulence factor.** *Mol Biochem Parasitol* 2002, **120**:33-40.
4. McGwire BS, O'Connell WA, Chang KP, Engman DM: **Extracellular release of the glycosylphosphatidylinositol (GPI)-linked *Leishmania* surface metalloprotease, gp63, is independent of GPI phospholipolysis: implications for parasite virulence.** *J Biol Chem* 2002, **277**:8802-8809.
5. Yao C, Donelson JE, Wilson ME: **The major surface protease (MSP or GP63) of *Leishmania* sp. Biosynthesis, regulation of expression, and function.** *Mol Biochem Parasitol* 2003, **132**:1-16.
6. Descoteaux A, Turco SJ: **The lipophosphoglycan of *Leishmania* and macrophage protein kinase C.** *Parasitol Today* 1993, **9**:468-471.
7. Beverley SM, Turco SJ: **Lipophosphoglycan (LPG) and the identification of virulence genes in the protozoan parasite *Leishmania*.** *Trends Microbiol* 1998, **6**:35-40.
8. Spath GF, Epstein L, Leader B, Singer SM, Avila HA, Turco SJ, et al: **Lipophosphoglycan is a virulence factor distinct from related glycoconjugates in the protozoan parasite *Leishmania major*.** *Proc Natl Acad Sci USA* 2000, **97**:9258-9263.
9. Garami A, Mehler A, Ilg T: **Glycosylation defects and virulence phenotypes of *Leishmania mexicana* phosphomannomutase and dolicholphosphate-mannose synthase gene deletion mutants.** *Mol Cell Biol* 2001, **21**:8168-8183.
10. Descoteaux A, Avila HA, Zhang K, Turco SJ, Beverley SM: ***Leishmania* LPG3 encodes a GRP94 homolog required for phosphoglycan synthesis implicated in parasite virulence but not viability.** *EMBO J* 2002, **21**:4458-4469.
11. Spath GF, Garraway LA, Turco SJ, Beverley SM: **The role(s) of lipophosphoglycan (LPG) in the establishment of *Leishmania major* infections in mammalian hosts.** *Proc Natl Acad Sci USA* 2003, **100**:9536-9541.
12. Gaur U, Showalter M, Hickerson S, Dalvi R, Turco SJ, Wilson ME, et al: ***Leishmania donovani* lacking the Golgi GDP-Man transporter LPG2 exhibit attenuated virulence in mammalian hosts.** *Exp Parasitol* 2009, **122**:182-191.
13. Pollock KG, McNeil KS, Mottram JC, Lyons RE, Brewer JM, Scott P, et al: **The *Leishmania mexicana* cysteine protease, CPB2.8, induces potent Th2 responses.** *J Immunol* 2003, **170**:1746-1753.
14. Buxbaum LU, Denise H, Coombs GH, Alexander J, Mottram JC, Scott P: **Cysteine protease B of *Leishmania mexicana* inhibits host Th1 responses and protective immunity.** *J Immunol* 2003, **171**:3711-3717.
15. Mahmoudzadeh-Niknam H, McKerrow JH: ***Leishmania tropica*: cysteine proteases are essential for growth and pathogenicity.** *Exp Parasitol* 2004, **106**:158-163.
16. Nourbakhsh F, Uliana SR, Smith DF: **Characterisation and expression of a stage-regulated gene of *Leishmania major*.** *Mol Biochem Parasitol* 1996, **76**:201-213.
17. Uliana SR, Goyal N, Freymuller E, Smith DF: ***Leishmania*: overexpression and comparative structural analysis of the stage-regulated *meta 1* gene.** *Exp Parasitol* 1999, **92**:183-191.
18. Ramos CS, Franco FA, Smith DF, Uliana SR: **Characterisation of a new *Leishmania* META gene and genomic analysis of the META cluster.** *FEMS Microbiol Lett* 2004, **238**:213-219.
19. Lawrence JG, Ochman H: **Amelioration of bacterial genomes: rates of change and exchange.** *J Mol Evol* 1997, **44**:383-397.
20. Lawrence JG, Ochman H: **Molecular archaeology of the *Escherichia coli* genome.** *Proc Natl Acad Sci USA* 1998, **95**:9413-9417.
21. Mrazek J, Karlin S: **Detecting alien genes in bacterial genomes.** *Ann N Y Acad Sci* 1999, **870**:314-329.
22. Opperdoes FR, Michels PA: **Horizontal gene transfer in trypanosomatids.** *Trends Parasitol* 2007, **23**:470-476.
23. Yang Z, Nielsen R: **Estimating synonymous and nonsynonymous substitution rates under realistic evolutionary models.** *Mol Biol Evol* 2000, **17**:32-43.
24. Dowd SE, Ishizaki H: **Microarray based comparison of two *Escherichia coli* O157:H7 lineages.** *BMC Microbiol* 2006, **6**:30.
25. Chuang SE, Blattner FR: **Characterization of twenty-six new heat shock genes of *Escherichia coli*.** *J Bacteriol* 1993, **175**:5242-5252.
26. Saar Y, Ransford A, Waldman E, Mazareb S, min-Spector S, Plumblee J, et al: **Characterization of developmentally-regulated activities in axenic amastigotes of *Leishmania donovani*.** *Mol Biochem Parasitol* 1998, **95**:9-20.
27. Debrabant A, Joshi MB, Pimenta PF, Dwyer DM: **Generation of *Leishmania donovani* axenic amastigotes: their growth and biological characteristics.** *Int J Parasitol* 2004, **34**:205-217.
28. Alcolea PJ, Alonso A, Gomez MJ, Sanchez-Gorostiaga A, Moreno-Paz M, Gonzalez-Pastor E, et al: **Temperature increase prevails over acidification in gene expression modulation of amastigote differentiation in *Leishmania infantum*.** *BMC Genomics* 2010, **11**:31.
29. Ginalski K, Rychlewski L: **Protein structure prediction of CASP5 comparative modeling and fold recognition targets using consensus alignment approach and 3D assessment.** *Proteins* 2003, **53**(Suppl 6):410-417.
30. Sali A, Blundell TL: **Comparative protein modelling by satisfaction of spatial restraints.** *J Mol Biol* 1993, **234**:779-815.
31. Holm L, Rosenström P: **Dali server: conservation mapping in 3D.** *Nucl Acids Res* 2010, **38**:545-549.
32. Hasegawa H, Holm L: **Advances and pitfalls of protein structural alignment.** *Curr Opin Struct Biol* 2009, **19**:341-348.
33. Schuch R, Maurelli AT: **MxiM and MxiJ, base elements of the Mxi-Spa type III secretion system of *Shigella*, interact with and stabilize the MxiD secretin in the cell envelope.** *J Bacteriol* 2001, **183**:6991-6998.
34. Schuch R, Maurelli AT: **The mxi-Spa type III secretory pathway of *Shigella flexneri* requires an outer membrane lipoprotein, MxiM, for invasive translocation.** *Infect Immun* 1999, **67**:1982-1991.
35. Lario PI, Pfuetzner RA, Frey EA, Creagh L, Haynes C, Maurelli AT, et al: **Structure and biochemical analysis of a secretin pilot protein.** *EMBO J* 2005, **24**:1111-1121.
36. Overath P, Stierhof YD, Wiese M: **Endocytosis and secretion in trypanosomatid parasites - Tumultuous traffic in a pocket.** *Trends Cell Biol* 1997, **7**: 27-33.
37. Grzyb J, Latowski D, Strzalka K: **Lipocalins - a family portrait.** *J Plant Physiol* 2006, **163**: 895-915.
38. Bates PA, Dwyer DM: **Biosynthesis and secretion of acid phosphatase by *Leishmania donovani* promastigotes.** *Mol Biochem Parasitol* 1987, **26**:289-296.

39. Bates PA, Hermes I, Dwyer DM: *Leishmania donovani*: immunochemical localization and secretory mechanism of soluble acid phosphatase. *Exp Parasitol* 1989, **68**:335-346.
40. Bates PA, Hermes I, Dwyer DM: Golgi-mediated post-translational processing of secretory acid phosphatase by *Leishmania donovani* promastigotes. *Mol Biochem Parasitol* 1990, **39**:247-255.
41. Cuvillier A, Redon F, Antoine JC, Chardin P, DeVos T, Merlin G, et al: LdARL-3A, a *Leishmania* promastigote-specific ADP-ribosylation factor-like protein, is essential for flagellum integrity. *J Cell Sci* 2000, **113**(Pt 11):2065-2074.
42. Parodi-Talice A, Araújo JM, Torres C, Pérez-Victoria JM, Gamarro F, Castanys S, et al: The overexpression of a new ABC transporter in *Leishmania* is related to phospholipid trafficking and reduced infectivity. *Biochim Biophys Acta* 2003, **1612**:195-207.
43. Sahin A, Espiau B, Tetaud E, Cuvillier A, Lartigue L, Ambit A, Robinson DR, Merlin G, et al: The *Leishmania* ARL-1 and Golgi traffic. *PLoS ONE* 2008, **3**: e1620.
44. Nara T, Hshimoto T, Aoki T: Evolutionary implications of the mosaic pyrimidine-biosynthetic pathway in eukaryotes. *Gene* 2000, **257**:209-222.
45. Molinas SM, Altabe SG, Oppendoes FR, Rider MH, Michels PA, Uttaro AD: The multifunctional isopropyl alcohol dehydrogenase of *Phytomonas* sp. could be the result of a horizontal gene transfer from a bacterium to the trypanosomatid lineage. *J Biol Chem* 2003, **278**:36169-36175.
46. Cazalet C, Rusniok C, Bruggemann H, Zidane N, Magnier A, Ma L, et al: Evidence in the *Legionella pneumophila* genome for exploitation of host cell functions and high genome plasticity. *Nat Genet* 2004, **36**:1165-1173.
47. Chien M, Morozova I, Shi S, Sheng H, Chen J, Gomez SM, et al: The genomic sequence of the accidental pathogen *Legionella pneumophila*. *Science* 2004, **305**:1966-1968.
48. de Felipe KS, Pampou S, Jovanovic OS, Pericone CD, Ye SF, Kalachikov S, et al: Evidence for acquisition of *Legionella* type IV secretion substrates via interdomain horizontal gene transfer. *J Bacteriol* 2005, **187**:7716-7726.
49. Annoura T, Nara T, Makiuchi T, Hashimoto T, Aoki T: The origin of dihydroorotate dehydrogenase genes of kinetoplastids, with special reference to their biological significance and adaptation to anaerobic, parasitic conditions. *J Mol Evol* 2005, **60**:113-127.
50. Whitaker JW, McConkey GA, Westhead DR: Prediction of horizontal gene transfers in eukaryotes: approaches and challenges. *Biochem Soc Trans* 2009, **37**:792-5.
51. Kobayashi H, Miyamoto T, Hashimoto Y, Kiriki M, Motomatsu A, Honjoh K, et al: Identification of factors involved in recovery of heat-injured *Salmonella Enteritidis*. *J Food Prot* 2005, **68**:932-941.
52. Liic M, Jovanovic M, Jovanovic G, Savic DJ: Identification of the CysB-regulated gene, hslJ, related to the *Escherichia coli* novobiocin resistance phenotype. *FEMS Microbiol Lett* 2003, **224**:239-246.
53. Ramos CS, Yokoyama-Yasunaka JK, Guerra-Giraldez C, Price HP, Mortara RA, Smith DF, et al: *Leishmania amazonensis* META2 protein confers protection against heat shock and oxidative stress. *Exp Parasitol* 2011, **127**:228-37.
54. Luo Y, Bertero MG, Frey EA, Pfuetzner RA, Wenk MR, Creagh L, et al: Structural and biochemical characterization of the type III secretion chaperones CesT and SigE. *Nat Struct Biol* 2001, **8**:1031-1036.
55. Birtalan SC, Phillips RM, Ghosh P: Three-dimensional secretion signals in chaperone-effector complexes of bacterial pathogens. *Mol Cell* 2002, **9**:971-980.
56. Keeling PJ, Palmer JD: Horizontal gene transfer in eukaryotic evolution. *Nat Rev Genet* 2008, **9**:605.
57. Whitaker JW, McConkey GA, Westhead DR: The transferome of metabolic genes explored: analysis of the horizontal transfer of enzyme encoding genes in unicellular eukaryotes. *Genome Biol* 2009, **10**:R36.
58. Wilson ME, Jeronimo SM, Pearson RD: Immunopathogenesis of infection with the visceralizing *Leishmania* species. *Microb Pathog* 2005, **38**:147-160.
59. Silverman JM, Clos J, deOliveira CC, Shirvani O, Fang Y, Wang C, et al: An exosome-based secretion pathway is responsible for protein export from *Leishmania* and communication with macrophages. *J Cell Sci* 2010, **123**:842-852.
60. Silverman JM, Clos J, Horakova E, Wang AY, Wiesgigl M, Kelly I, et al: *Leishmania* exosomes modulate innate and adaptive immune responses through effects on monocytes and dendritic cells. *J Immunol* 2010, **185**:5011-5022.
61. Altschul SF, Madden TL, Schaffer AA, Zhang J, Zhang Z, Miller W, et al: Gapped BLAST and PSI-BLAST: a new generation of protein database search programs. *Nucleic Acids Res* 1997, **25**:3389-3402.
62. Finn RD, Mistry J, Tate J, Coggill P, Heger A, Pollington JE, et al: The Pfam protein families database. *Nucleic Acids Res* 2010, **38**:D211-D222.
63. Pei J, Kim BH, Grishin NV: PROMALS3D: a tool for multiple protein sequence and structure alignments. *Nucleic Acids Res* 2008, **36**:2295-2300.
64. Jain R, Ramineni S, Parekh N: Integrated Genomic Island Prediction Tool (IGIPT). *IEEE Proceedings of International Conference on Information Technology (ICIT2008)*, icit 2008, 131-132.
65. Chanda I, Pan A, Saha SK, Dutta C: Comparative codon and amino acid composition analysis of Trityps-conspicuous features of *Leishmania major*. *FEBS Lett* 2007, **581**:5751-5758.
66. Sharp PM, Li WH: The Codon Adaptation Index—a measure of directional synonymous codon usage bias, and its potential applications. *Nucleic Acids Res* 1987, **15**:1281-1295.
67. Edgar RC: MUSCLE: multiple sequence alignment with high accuracy and high throughput. *Nucleic Acids Res* 2004, **32**:1792-1797.
68. Guindon S, Dufayard JF, Lefort V, Anisimova M, Hordijk W, Gascuel O: New Algorithms and Methods to Estimate Maximum-Likelihood Phylogenies: Assessing the Performance of PhyML 3.0. *Systematic Biology* 2010, **59**:307-21.
69. Abascal F, Zardoya R, Posada D: ProtTest: Selection of best-fit models of protein evolution. *Bioinformatics* 2005, **21**:2104-2105.
70. Letunic I, Bork P: Interactive Tree Of Life v2: online annotation and display of phylogenetic trees made easy. *Nucleic Acids Res* 2011.
71. Yang Z: PAML: a program package for phylogenetic analysis by maximum likelihood. *Comput Appl Biosci* 1997, **13**:555-556.
72. Jones TA, Zou JY, Cowan SW, Kjeldgaard M: Improved methods for building protein models in electron density maps and the location of errors in these models. *Acta Crystallogr A* 1991, **47**(Pt 2):110-119.
73. DeLano WL: *The PyMol molecular graphics system* San Carlos, CA: DeLano Scientific LLC; 2004.
74. Bera A, Singh S, Nagaraj R, Vaidya T: Induction of autophagic cell death in *Leishmania donovani* by antimicrobial peptides. *Mol Biochem Parasitol* 2003, **127**:23-35.
75. Chomczynski P, Sacchi N: The single-step method of RNA isolation by acid guanidinium thiocyanate-phenol-chloroform extraction: twenty-something years on. *Nat Protoc* 2006, **1**:581-585.
76. Tupperwar N, Vineeth V, Rath S, Vaidya T: Development of a real-time polymerase chain reaction assay for the quantification of *Leishmania* species and the monitoring of systemic distribution of the pathogen. *Diagn Microbiol Infect Dis* 2008, **61**:23-30.
77. Kapler GM, Coburn CM, Beverley SM: Stable transfection of the human parasite *Leishmania major* delineates a 30-kilobase region sufficient for extrachromosomal replication and expression. *Mol Cell Biol* 1990, **10**:1084-1094.
78. Rasband WS: *ImageJ*. US National Institutes of Health, Bethesda, Maryland, USA; 1997 [http://imagej.nih.gov/ij/].

doi:10.1186/1471-2148-11-334

Cite this article as: Puri et al.: Evolutionary and functional insights into *Leishmania* META1: evidence for lateral gene transfer and a role for META1 in secretion. *BMC Evolutionary Biology* 2011 **11**:334.

Submit your next manuscript to BioMed Central and take full advantage of:

- Convenient online submission
- Thorough peer review
- No space constraints or color figure charges
- Immediate publication on acceptance
- Inclusion in PubMed, CAS, Scopus and Google Scholar
- Research which is freely available for redistribution

Submit your manuscript at
www.biomedcentral.com/submit

